Neural Network AEROsol Retrieval for Geostationary Satellite (NNAeroG): Algorithm Framework Development

Xingfeng Chen[1], Fengjie Zheng[2], Lili Wang[3], Limin Zhao[1], Jiaguo Li[1], Gerrit de Leeuw[4,1,5,6], Lei Li[7], Kainan Zhang[8], Lu She[9], Kaitao Li[1], Zhengqiang Li[1]

[1]Aerospace Information Research Institute, Chinese Academy of Sciences, Beijing, China

[2]Space Engineering University, Beijing, China

[3]State Key Laboratory of Atmospheric Boundary Layer Physics and Atmospheric Chemistry (LAPC), Institute of Atmospheric Physics, Chinese Academy of Sciences, Beijing, China

[4]Royal Netherlands Meteorological Institute (KNMI), R&D Satellite Observations, De Bilt, The Netherlands

[5]Nanjing University of Information Science & Technology (NUIST). School of Atmospheric Physics, Nanjing, China

[6]University of Mining and Technology (CUMT), School of Environment Science and Spatial Informatics, Xuzhou, China

[7]State Key Laboratory of Severe Weather (LASW), Key Laboratory of Atmospheric Chemistry (LAC), Chinese Academy of Meteorological Sciences, CMA, Beijing, China

[8]School of Geology Engineering and Geomatics, Chang'an University, Xi'an, China

[9]College of Resources and Environmental Science, Ningxia University, Yinchuan, China

Corresponding author: G. de Leeuw (gerrit.de.leeuw@knmi.nl) and L. Li (lilei@cma.gov.cn)

Key Points:

- Propose a machine learning framework for aerosol retrieval from geostationary satellite
- AOD, FMF and AE can be retrieved with high accuracy
- Thermal infrared spectral bands were used for aerosol retrieval

Abstract

Geostationary satellites observe the earth surface and atmosphere with a short repeat time which can thus provide aerosol parameters with high temporal resolution. Due to the limited information content in satellite data, and the coupling between the signals received from the surface and the atmosphere, the accurate retrieval of multiple aerosol parameters over land is difficult. Here we propose a Neural Network AEROsol retrieval framework for Geostationary satellite (NNAeroG) which can potentially be applied to different instruments to retrieve various aerosol parameters. NNAeroG was applied for aerosol retrieval using data from the Advanced Himawari Imager on Himawari-8 and the results were evaluated versus independent ground-based sun photometer reference data. The retrieved Aerosol Optical Depth, Ångström Exponent and Fine Mode Fraction are significantly better than the official JAXA aerosol products. The use of thermal infrared bands is meaningful for aerosol retrieval.

Plain Language Summary

Atmospheric aerosol particles have a large influence on the Earth' climate, on air quality, human health and many different processes in the atmosphere. The amount and the size of aerosol particles are important. Satellite-based optical sensors can be used to observe aerosol properties, by the detection of solar radiation reflected by the particles at different wavelengths and in different directions. The radiation reflected by aerosols needs to be separated from the reflection from the Earth surface. Methods have been developed to achieve this, over different types of surfaces. Most satellites used for aerosol detection, observe any location on Earth only once per day. Geostationary satellite can observe the earth many times each day. We successfully developed a method to obtain information on both the amount of aerosols and the size of the particles using geostationary satellite observations in a neural network method named NNAeroG.

1 Introduction

Atmospheric aerosols have key influences on global climate and environment (Kaufman et al., 2002). Measurements using ground-based instruments can provide a multitude of aerosol parameters which together characterize the aerosol microphysical and chemical properties in great detail and with high accuracy. Ground-based measurements however apply to local conditions with a limited spatial extend. In contrast, satellite measurements using radiometers

can provide aerosol information over large spatial scales with global coverage (Levy et al., 2013), but for less parameters, with less detail and lower accuracy. The use of space-borne radiometers to obtain aerosol information from the radiances or reflectances measured at the Top Of the Atmosphere (TOA), requires the development of retrieval methods based on radiative transfer models. To optimally use the sensor characteristics, such as multiple wavelengths, multiple views and polarization information, different types of algorithms have been developed. For sensors in a Sun-synchronous orbit, algorithms such as Dark Target (DT) (Levy et al., 2013), Deep Blue (DB) (Hsu et al., 2006), Multi-Angle Implementation of Atmospheric Correction (MAIAC) (Lyapustin et al., 2011), AATSR dual-view (ADV) (Kolmonen et al., 2016), MISR aerosol retrieval method (Kahn and Gaitley, 2015), Generalized Retrieval of Aerosol and Surface Properties (GRASP) (Dubovik et al., 2011), etc., have been developed to retrieve aerosol properties from different sensors. Sensors in a sun-synchronous orbit may offer near-daily global coverage (e.g. MODIS, VIIRS, POLDER, MERIS) or in several days (MISR, AATSR, SLSTR), depending on their swath. Geostationary satellites view a specific part of the Earth but with high temporal resolution which can thus be used to provide aerosol information suitable to track the evolution of aerosol properties (Sowden et al., 2019). Methods to retrieve aerosol properties from geostationary satellites have been developed, such as GOCI Yonsei Aerosol Retrieval (YAER) (Choi et al., 2016), for MSG/SEVIRI (Bennouna et al., 2009; Govaerts and Lufarelli, 2018) and the Advanced Himawari Imager (AHI) on Himawari-8 which is the subject of this paper.

A number of aerosol retrieval methods were developed for Himawari-8/AHI. The official aerosol products of AHI, available from the Japan Aerospace Exploration Agency (JAXA), are retrieved by a DB-type method (Yoshida et al., 2018). Ge et al. (2018) proposed a DT method for Himawari-8/AHI aerosol retrieval by defining a new Normalized Difference Vegetation Index (NDVI) calculated from the 0.86 μm and 2.3 μm wavebands; the retrieved AOD had an R^2 of 0.81with ground-based network measurements. Yan et al. (2018) proposed a minimum albedo aerosol retrieval method (MAARM) to retrieve AOD, Ångström Exponent (AE) and Fine Mode Fraction (FMF). However, the accuracies of AE and FMF were not high. Recently, Su et al. (2021) proposed a High-Precision Aerosol Retrieval Algorithm (HiPARA) which employs a monthly spectral reflectance ratio library and aerosol type from Aerosol Robotic Network (AERONET) statistics to retrieve AOD. Gao et al. (2021) improved the surface reflectance estimation of the DT method by taking into account the land cover, NDVI and scattering angle.

The retrieved AOD in the study of Su et al. (2021) and Gao et al. (2021) has a better accuracy than the JAXA AOD. Huttunen et al. (2016) compared 6 methods of AOD retrieval including one radiative transfer modeling LUT (Look Up Table) method, one non-linear regression method and four machine learning methods and learned that the LUT method assumes parameters such as Single Scattering Albedo (SSA) which introduced more uncertainties into the products, whereas, the machine learning methods did not use any assumptions and their performance was better.

Machine learning has been used as a new technique to solve the complicated aerosol retrieval problems with good results. Chen et al. (2020) proposed a Neural Network AEROsol (NNAero) retrieval method for the use with MODerate resolution Imaging Spectroradiometer (MODIS) data, which could jointly retrieve AOD and FMF with a significant improvement of accuracy. For Himawari-8/AHI, She et al. (2020) trained a deep neural network by AERONET observations to retrieve AOD using reflectances in 6 wavebands, and achieved better AOD accuracy than JAXA AOD.

In this paper, a framework for a Neural Network AEROsol Retrieval algorithm for Geostationary Satellite (NNAeroG) is presented based on the work of Chen et al. (2020). In contrast to sun-synchronous satellites, a geostationary satellite like Himawari-8 provides multiple observations over the same location which can be used in time series algorithms (e.g., Li et al., 2020). Like aerosol retrieval algorithms mentioned above, Chen et al. (2020) and She et al. (2020) used only reflective spectral bands covering the visible and near infrared (VNIR) and the shortwave infrared (SWIR) parts of the solar spectrum. In fact, efforts to include thermal infrared (TIR) bands for aerosol retrieval have been made for aerosol type (Clarisse et al., 2013) and dust aerosol (Sowden and Blake, 2020). For the use of TIR wavelengths, only the radiance at TOA is needed which circumvents problems associated with separation of the aerosol and surface contributions. The use of time series and TIR wavelengths constitutes a substantial improvement of NNAeroG as compared with NNAero. For the neural network training and validation, the output data were extracted which are available from sun photometers in the AERONET (Holben et al., 1998) and Sun–Sky Radiometer Observation Network (SONET) (Li et al., 2018) networks. The study area is China. The importance of input features (spectral bands and geometric angles) was given using the Extreme Gradient Boosting (XGBoost) model (Gui et al., 2020).

2 Materials

2.1 Himawari-8/AHI data

Himawari-8 is a Japanese weather satellite which was launched on 7 October 2014 in a geostationary orbit at a height of 35793 km at 140.7°E, with a spatial coverage of 150° by 150°. The primary instrument onboard Himawari-8 is the Advanced Himawari Imager (AHI) which measures upwelling radiation at TOA in 16 spectral bands (listed in Table S1 in the supporting information) with a spatial resolution down to 500 m every 10 minutes (fullldisk). AHI solar zenith angle, viewing zenith angle, relative azimuth angle (solar azimuth angle minus viewing azimuth angle), TOA reflectances in 6 VNIR and SWIR bands and brightness temperatures in 10 TIR bands were collected for each cloud-free pixel. Thus, in total 19 features are available and some of them will be selected for retrieval by XGBoost. In this study, level 1 data and aerosol products data during the years of 2016 - 2019 were used.

The AHI data formatted in netCDF were downloaded from the JAXA "P-Tree" system (ftp://ftp.ptree.jaxa.jp). The AHI level 1 calibrated data are gridded in pixels of 0.02º and contain the Earth surface albedo measured at TOA in bands 1-6, and the brightness temperatures measured at TOA in bands 7-16. We calculated the reflectances from the Level 1 albedo in bands 1-6 using

$$\rho_\lambda = \frac{\alpha_\lambda}{cos(\theta_s)} \quad (1)$$

where ρ_λ is the TOA reflectance at wavelength λ, α_λ is the TOA albedo, and θ_s is the solar zenith angle.

JAXA aerosol products of Himawari-8/AHI are also available from the "P-Tree" system. The JAXA aerosol product is gridded in pixels of 0.05º and contain AOD, AE and FMF. Cloud products available in P-Tree are used to select cloud-free pixels (Shang et al., 2017).

2.2 Ground-based data and study area

Reference aerosol products for the training of the NNAeroG and the validation of the results were obtained from two sun photometer networks in China, i.e. AERONET and SONET. The level 2.0 data of AERONET (Version 3.0) and SONET were used in this study. The mean values of AOD, AE, FMF over ± 30 min from the satellite imaging time were extracted to match

the satellite data at the same location (Levy et al., 2013) with spatial match as shown in Table S1. Data from 12 AERONET sites and 16 SONET sites (not common with the 12 AERONET sites) during the years of 2016 - 2019 were collected. All sites are indicated in Figure S1. The Himawari-8/AHI covers all China except for a small part west of 80°E. Only land surfaces in China covered by AHI were considered in this paper.

3 Algorithm framework development

3.1 Algorithm framework strategy

The geostationary satellite data have three dimensions (spectral, spatial, and temporal information) that could be used to constrain aerosol retrieval. In Chen et al. (2020), the retrieval of MODIS AOD and FMF were achieved using the spectral and spatial information. Here we propose the NNAeroG with all three dimensions. The flowchart of the NNAeroG algorithm framework is shown in Figure 1.

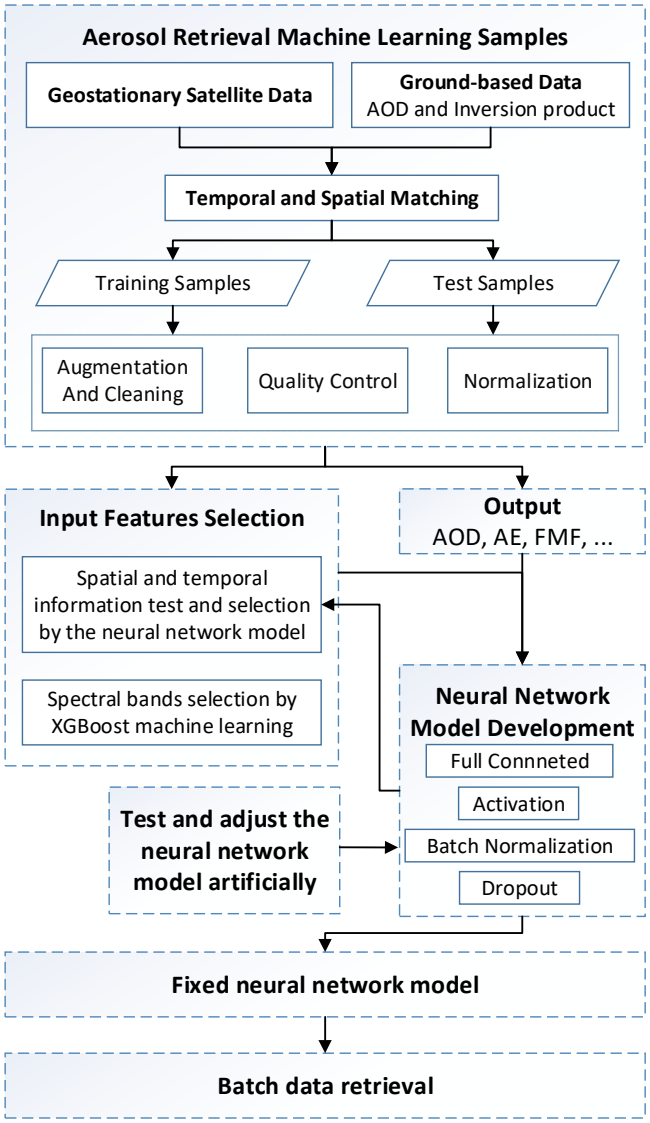

Figure 1. Flowchart of NNAeroG algorithm.

In the first step, the machine learning samples for neural network model training and validation, including the geostationary satellite data as input and the ground-based data as output, were prepared. After temporal and spatial matching, all samples were divided into two parts, training and validation, to ensure that the validation samples are independent of the training samples. As shown in Figure S1, sites with their names in red were selected for independent validation. And then, data augmentation produces more samples to create a uniform distribution. For example, there are less samples with FMF < 0.2 which would lead to a lack of learning for coarse aerosols, so we can copy these samples, with addition of 2% Gaussian noise, as augmentation. It is noted that quality control can filter unsuitable data such as cloud-

contaminated pixels. Every input value would be transferred in [0, 1] to obtain good fitting results of neural network.

In the second step, the geostationary data in one sample has multi-spectral, multi-temporal and multi-pixels (sub-image centered on the site). Which one is the important feature for the aerosol retrieval? Radiative transfer theory and previous aerosol retrieval algorithms can provide optional preferences. At the same time, the decision tree based XGBoost machine learning method can provide the importance value of each input feature.

In the third step, to establish a machine learning model, the neural network is recommended for its excellent non-linear fitting ability (Yan et al., 2020; She et al., 2020). More important, XGBoost, which is based on the decision tree with thresholds, has a potential capability to select which is the important feature for retrieval from spectral bands.

In the fourth step, the NNM was developed. Temporal and spatial information were selected according to the NNM test results. The number of input features N were defined by:

$$N = round({S_{pix}}^2 \times R_{Dark}) \times T \times N_{SB} \quad (2)$$

Where S_{pix} is the side length of the pixels square in the satellite image centered over each ground-based site, here $S_{\mathrm{pix}} \leq 7$ with the assumption that aerosol is homogeneous over an area of less than 14 km × 14 km. R_{Dark} is the ratio of the dark and clear-sky pixels in each area of $S_{\mathrm{pix}} \times S_{\mathrm{pix}}$ pixels. The darkness order of pixels is given by the TOA reflectance at 2.3 μm which is used to enhance the number of pixels with a relatively large atmospheric contribution to the TOA signal by selecting pixels with the darkest surface. N_{SB} (≤19) is the number of features selected by XGBoost from the 19 angles, spectral reflectances and brightness temperatures, in the second step. T is the number of temporal satellite data, here $T = 1$ or 3.

In the fifth step, the NNM was trained by the selected spectral, spatial and temporal input features. With the independent test (also validation), the architecture and its parameters of NNM were fixed.

Finally, the fixed NNM could be used to predict (or retrieve) aerosol with large amount of remote sensing data.

3.2 Neural network model

A neural network shows better performance for nonlinear regression than other machine learning methods such as XGBoost and RF (Random Forest) (Yan et al., 2020). We also tested

different machine learning methods, but the neural network was selected for NNAeroG because of the best performance. The NNM architecture for NNAeroG was designed as shown in Figure S2.

In the full connected layer (FC), the basic unit is neuron (blue circle in Figure S2), which is a weighted summation of its inputs. The output of a neuron is expressed as

$$z = \sum_{i=1}^{m} \omega_i * x_i \quad (3)$$

where ω_i is the weighting coefficient for the input x_i. The training process is to obtain the best ω_i to achieve the best prediction accuracy. In Figure S2, the NNM is composed of three parts: input, hidden layers and output.

3.3 Application to Himawari-8/AHI and comparison with NNAero

The development of NNAeroG is based on the NNAero algorithm designed for MODIS FMF retrieval (Chen et al., 2020). Because of the differences between the AHI and MODIS sensors, NNAero cannot be directly applied to AHI. Therefore, for the development of NNAeroG the following changes were introduced.

The Himawari-8/AHI data have lower spatial resolution and higher temporal resolution as compared to MODIS. For the application of NNAeroG on Himawari-8/AHI, the settings of NNAeroG on Himawari-8 and comparisons with NNAero on MODIS are presented in Table S2.

Compared with NNAero, NNAeroG employs separated NNM for every aerosol parameter retrieval. The FCNN architecture employed in NNM is not sensitive to the shape or texture characteristics of the ground-based site. Samples from a single site collected at different times are independent. Therefore, the independent validation (or test) data from sites which were not used for training are not necessary. However, to ensure strictly independent validation, in this study data from sites used for training were not used for validation. The input satellite data only include TOA reflectances and brightness temperatures, but no surface reflectances. All advantages of NNAeroG are shown in Table S2 as bold font.

4 Result and discussion

4.1 Selection of input features

The importance of each of the AHI input features was analyzed by XGBoost. The results of this analysis are presented in Figure 2, which shows that for the retrieval of AOD with the NNM, the 6.2μm, 6.9μm, 8.6μm, 11.2μm, 12.4μm wavelength bands have the lowest importance; therefore these bands were not used as input. For the retrieval of AE and FMF there is no significant difference between the input features which were thus all retained.

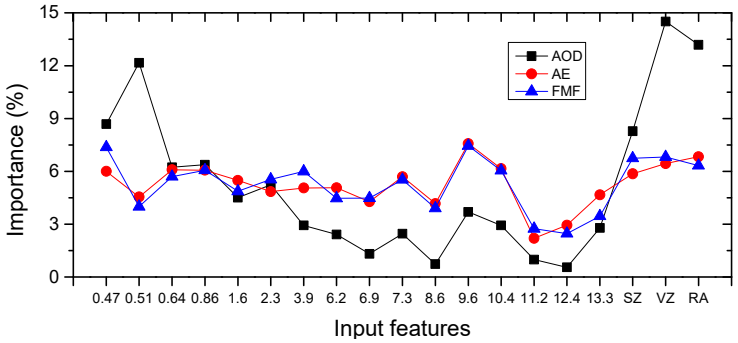

Figure 2. Aerosol retrieval importance of Himawari-8/AHI input features. The numbers on the horizontal axis are spectral bands in μm. SZ, VZ and RA are solar zenith angle, viewing zenith angle and relative azimuth angle respectively.

According to Eq. 2, the spatial (S_{pix}, R_{Dark}) and temporal information (T) was tested by NNMs for AOD, AE and FMF. Assuming that AE and FMF do not change during 20 min, 3 AHI images (±10 min around the sun photometer measurement) were used together as input in the retrieval. The settings are shown in Table 1.

Table 1. Spectral, spatial and temporal settings for NNAeroG retrieval using Himawari-8/AHI data

Aerosol parameter	**Spectral and angles**	**Spatial** (pixel)	**Temporal**	**N in Eq.2**
AOD	11 bands + 3 angles	1	single	14
AE	16 bands + 3 angles	Round(7^2×0.5) = 25	3 observations	475
FMF	16 bands + 3 angles	Round(5^2×0.4) = 10	3 observations	190

4.2 Validation

For strictly independent validation, the test dataset needs to include only samples from the ground-based sites which were not used in the NNM training (Chen et al., 2020; She et al.,

2020). Scatterplots of the AOD, AE and FMF retrieved using NNAeroG versus AERONET and SONET reference data are presented in Figure 3, for both the training data set and the independent validation data set. Also shown are similar plots for the JAXA operational data. It is noted that in Figure 3 the spatial resolution for the JAXA products is 5 km and for the NNAeroG-retrieved data it is 2 km.

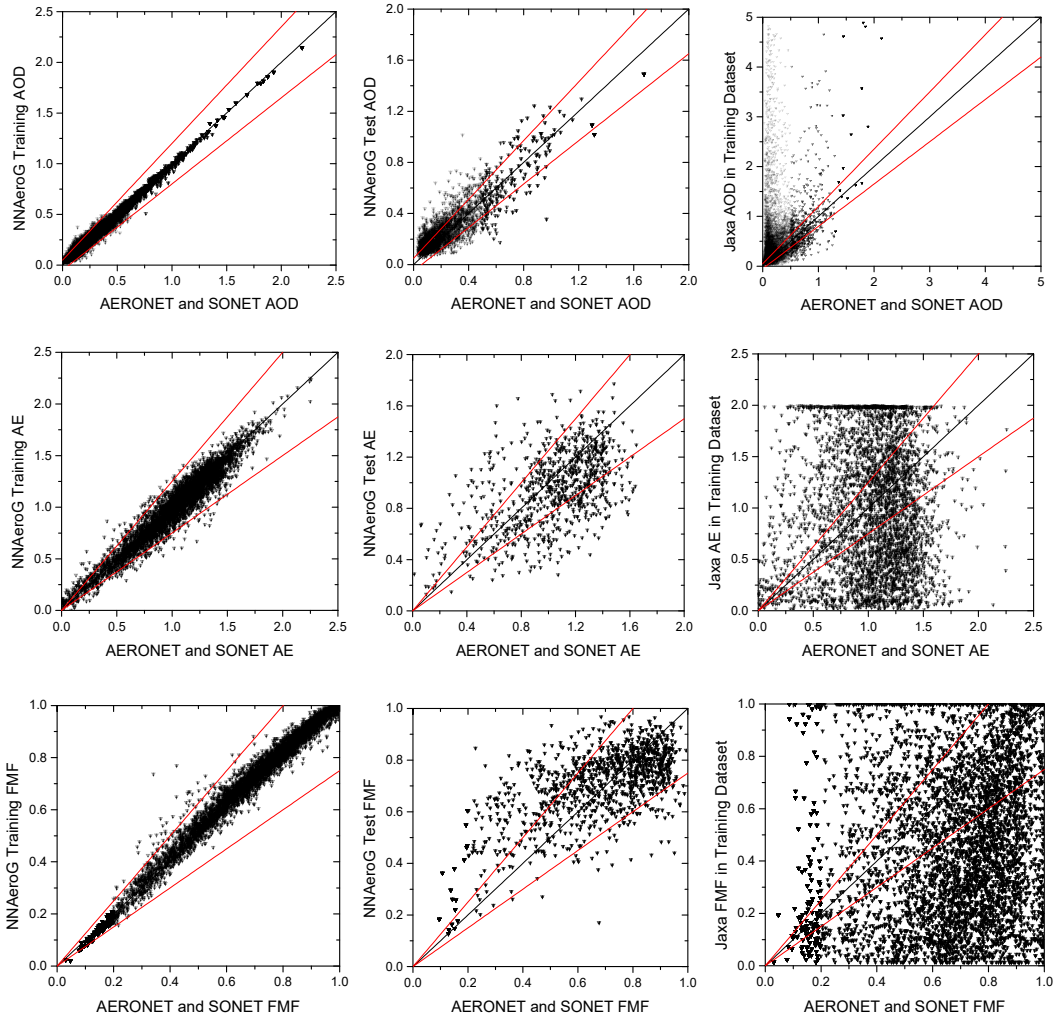

Figure 3. Scatterplots of Himawari-8/AHI retrieved AOD, AE and FMF versus AERONET and SONET reference data. The left column shows scatterplots for NNAeroG products over the training sites, i.e. versus the same data that were used for training the NNM. The middle column shows scatterplots for NNAeroG products over sites that were not used in the NNM training. Scatterplots for the JAXA products are presented in the right column. The red lines are the EE envelopes for AOD, AE and FMF of ± (0.05 + 15%), ± 25% and ± 25%, respectively.

The scatterplots in Figure 3, middle column, show that for the NNAeroG retrievals over the validation sites, 63.7% of the AOD data are within the EE envelope of ± (0.05 + 15%), 60.9% of the AE and 65.6% of the FMF are within the EE of ± 25%. The data in Figure 3 and the statistical metrics for the comparison of the NNAeroG and JAXA products in Table S3 show the significant improvement of the retrieval accuracy of the NNAeroG AOD, AE and FMF products over those from the JAXA algorithm. Note however, that NNAeroG overestimates the AOD and FMF, and underestimates the AE. The values of RMSE, MAE, R^2 and R indicate the better accuracy for AOD than for than AE and FMF.

4.3 High temporal resolution products

Using the trained NNMs of NNAeroG, time series of aerosol parameters can be retrieved. Hourly high temporal resolution aerosol products (AOD, AE, and FMF) for September 20, 2020, from 01:00 to 10:00, are presented in Figure S3, which shows that the high spatial and temporal resolution of the NNAeroG retrievals provide detailed information on the spatial distribution of the aerosol properties and their temporal evolution. Specifically, from UTC 01:00 to 07:00, the AOD decreases over the North China Plain (NCP) and the area toward the Mongolia border, whereas the coverage increases. At the same time, the FMF over the NCP and to the north of the NCP increased indicating stronger dominatin of fine mode particles. The data in Figure S3 show that the high spatial and temporal resolution is helpful for monitoring the evolution of regional air quality.

5 Conclusions

The NNAeroG algorithm framework is proposed for aerosol retrieval using data from geostationary satellites. In the development of the framework, the satellite spectral, spatial and temporal information were selected using the decision tree machine learning method, which can help to filter the important input features. The spectral information is the most important input for AOD retrieval using the machine learning method. Because more observations are needed to constrain AE and FMF retrievals, more spatial pixels, 3 consecutive observations within 20 minutes, and all spectral bands, including TIR bands, are jointly used as input. Then, the neural network model for each aerosol parameter retrieval was developed and trained by using both geostationary satellite and ground-based data.

After training was completed, the NNAeroG was applied to Himawari-8/AHI data to produce AOD, AE and FMF retrievals with 2 km spatial resolution and 10 min temporal resolution. The results were validated against independent reference data from the AERONET and SONET sun photometer networks. The validation results show that the accuracy of the NNAeroG aerosol products is significantly better than that of the JAXA version 2.1 aerosol products. The NNAeroG results indicate that the geostationary satellite data can be used to retrieve aerosol with higher accuracy not only for AOD but also for other parameters.The proposed NNAeroG provides a generic aerosol retrieval framework which also has a potential for application to other geostationary satellites such as FengYun-4.

Acknowledgments

This study is supported by the National Key Research and Development Program of China (No. 2019YFE0126600, No. 2019YFC0214603, No. 2016YFC1400900), and the 13th Five-Year Plan of Civil Aerospace Technology Advanced Research Projects of China. The study contributes to the ESA / MOST cooperation project DRAGON5, Topic 3 Atmosphere, sub-topic 3.2 Air-Quality. The authors acknowledge Himawari-8/AHI data system (P-Tree) SONET and AERONET groups for the satellite and ground-based data.

Data Availability Statement

AERONET and Himawari-8/AHI data sets used in this study are accessible at https://aeronet.gsfc.nasa.gov and ftp://ftp.ptree.jaxa.jp, respectively. SONET data are available on request from http://www.sonet.ac.cn.

References

Bennouna, Y. S., de Leeuw, G., Piazzola, J. & Kusmierczyk-Michulec, J. (2009). Aerosol remote sensing over the ocean using MSG-SEVIRI visible images. *Journal of Geophysical Research: Atmospheres*, *114*, D23203. https://doi.org/10.1029/2008JD011615

Chen, X., de Leeuw, G., Arola, A., Liu, S., Liu, Y., Li, Z. & Zhang, K. (2020). Joint retrieval of the aerosol fine mode fraction and optical depth using MODIS spectral reflectance over northern and eastern China: Artificial neural network method. *Remote Sensing of Environment*, *249*, 112006. https://doi.org/10.1016/j.rse.2020.112006

Choi, M., Kim, J., Lee, J., Kim, M., Park, Y. J., Jeong, U., et al. (2016). GOCI Yonsei Aerosol retrieval (YAER) algorithm and validation during the DRAGON-NE Asia 2012 campaign. *Atmospheric Measurement Techniques*, *9*, 1377–1398. https://doi.org/10.5194/amt-9-1377-2016

Clarisse, L., Coheur, P.-F., Prata, F., Hadji-Lazaro, J., Hurtmans, D., & Clerbaux, C. (2013). A unified approach to infrared aerosol remote sensing and type specification. *Atmospheric Chemistry and Physics*, *13*: 2195–2221. https://doi.org/10.5194/acp-13-2195-2013

Dubovik, O., Herman, M., Holdak, A., Lapyonok, T., Tanré, D., Deuzé, J. L., et al. (2011). Statistically optimized inversion algorithm for enhanced retrieval of aerosol properties from spectral multi-angle polarimetric satellite observations. *Atmospheric Measurement Techniques*, *4*, 975–1018. https://doi.org/10.5194/amt-4-975-2011

Gao, L., Chen, L., Li, J., Li, C. & Zhu, L. (2021). An improved dark target method for aerosol optical depth retrieval over China from Himawari-8. *Atmospheric Research*, *250*, 105399. https://doi.org/10.1016/j.atmosres.2020.105399

Ge, B., Li, Z., Liu, L., Yang, L., Chen, X., Hou, W. & Qie, L. (2018). A dark target method for Himawari-8/AHI aerosol retrieval: Application and validation. *IEEE Transactions on Geoscience and Remote Sensing*, *57* (1), 381–394. https://doi.org/10.1109/TGRS.2018.2854743

Govaerts, Y. & Luffarelli, M. (2018). Joint retrieval of surface reflectance and aerosol properties with continuous variation of the state variables in the solution space – Part 1: theoretical concept. *Atmospheric Measurement Techniques*, *11*, 6589-6603. https://doi.org/10.5194/amt-11-6589-2018

Gui, K., Che, H., Zeng, Z., Wang, Y., Zhai, S., Wang, Z., et al. (2020). Construction of a virtual PM2.5 observation network in China based on high-density surface meteorological observations using the Extreme Gradient Boosting model. *Environment International*, *141*, 105801. https://doi.org/10.1016/j.envint.2020.105801

Holben, B.N., Eck, T.F., Slutsker, I., Tanre, D., Buis, J.P., Setzer, A., et al. (1998). AERONET—A federated instrument network and data archive for aerosol characterization. *Remote Sensing of Environment*, *66*, 1–16. https://doi.org/10.1016/S0034-4257(98)00031-5

Hsu, N.C., Tsay, S.C., King, M.D. & Herman, J.R. (2006). Deep blue retrievals of Asian aerosol properties during ACE-Asia. *IEEE Transactions on Geoscience and Remote Sensing*, *44* (11), 3180–3195. https://doi.org/10.1109/TGRS.2006.879540

Huttunen, J., Kokkola, H., Mielonen, T., Mononen, M.E.J., Lipponen, A., Reunanen, J., et al. (2016). Retrieval of aerosol optical depth from surface solar radiation measurements using machine learning algorithms, non-linear regression and a radiative transfer-based look-up table. *Atmospheric Chemistry and Physics*, 16, 8181–8191. https://doi.org/10.5194/acp-16-8181-2016

Kahn, R.A. & Gaitley, B.J. (2015). An analysis of global aerosol type as retrieved by MISR. *Journal of Geophysical Research: Atmospheres*, *120* (9), 4248–4281. https://doi.org/10.1002/2015JD023322

Kaufman, Y.J., Tanre, D. & Boucher, O. (2002). A satellite view of aerosols in the climate system. *Nature*, *419*, 215–223. https://doi.org/10.1038/nature01091

Kolmonen, P., Sogacheva, L., Virtanen, T. H., de Leeuw, G. & Kulmala, M.. (2016). The ADV/ASV AATSR aerosol retrieval algorithm: current status and presentation of a full-mission AOD data set. International Journal of Digital Earth, *9*(6), 545–561. https://doi.org/10.1080/17538947.2015.1111450

Levy, R.C., Mattoo, S., Munchak, L.A., Remer, L.A., Sayer, A.M., Patadia, F. & Hsu, N.C. (2013). The collection 6 MODIS aerosol products over land and ocean. *Atmospheric Measurement Techniques*, 6, 2989–3034. https://doi.org/10.5194/amt-6-2989-2013

Li, D., Qin, K., Wu, L., Mei, L., de Leeuw, G., Xue, Y., et al. (2020). Himawari-8-Derived Aerosol Optical Depth Using an Improved Time Series Algorithm Over Eastern China. *Remote Sensing,*, *12*, 978; https://doi.org/10.3390/rs12060978.

Li, Z.Q., Xu, H., Li, K.T., Li, D.H., Xie, Y.S., Li, L., et al. (2018). Comprehensive study of optical, physical, chemical, and radiative properties of total columnar atmospheric aerosols over China: an overview of sun–sky radiometer observation network (SONET) measurements. *Bulletin of the American Meteorological Society*, *99* (4), 739–755. https://doi.org/10.1175/BAMS-D-17-0133.1

Lyapustin, A., Wang, Y., Laszlo, I., Kahn, R., Korkin, S., Remer, L., et al. (2011). Multiangle implementation of atmospheric correction (MAIAC): 2. Aerosol algorithm. *Journal of Geophysical Research: Atmospheres*, *116*, D03211. https://doi.org/10.1029/2010JD014985

Shang, H., Chen, L., Letu, H., Zhao, M., Li, S. & Bao, S. (2017). Development of a daytime cloud and haze detection algorithm for Himawari-8 satellite measurements over central and eastern China. *Journal of Geophysical Research: Atmospheres*, *122*, D025659. https://doi.org/10.1002/2016JD025659

She, L., Zhang, H., K., Li, Z., de Leeuw, G. & Huang, B. (2020). Himawari-8 aerosol optical depth (AOD retrieval using a deep neural network trained using AERONET observations. *Remote Sensing*, *12*(24), 4125. https://doi.org/10.3390/rs12244125

Sowden, M. & Blake, D. (2020). Which dual-band infrared indices are optimum for identifying aerosol compositional change using Himawari-8 data? *Atmospheric Environment*, *241*, 117620. https://doi.org/10.1016/j.atmosenv.2020.117620

Sowden, M., Mueller, U. & Blake, D. (2019). What temporal resolution is required for remote sensing of regional aerosol concentrations using the Himawari-8 geostationary satellite. *Atmospheric Environment*, *216*, 116914. https://doi.org/10.1016/j.atmosenv.2019.116914

Yan, X., Li, Z., Luo, N., Shi, W., Zhao, W., Yang, X. & Jin, J. (2018). A minimum albedo aerosol retrieval method for the new-generation geostationary meteorological satellite Himawari-8. *Atmospheric Research*, *207*, 14-27. https://doi.org/10.1016/j.atmosres.2018.02.021

Yan, X., Liang, C., Jiang, Y., Luo, N., Zang, Z. & Li, Z. (2020). A deep learning approach to improve the retrieval of temperature and humidity profiles from a ground-based microwave radiometer. *IEEE Transactions on Geoscience and Remote Sensing*, *58*(12), 842-8437. https://doi.org/10.1109/TGRS.2020.2987896

Yoshida, M., Kikuchi, M., Nagao, T.M., Murakami, H., Nomaki, T. & Higurashi, A. (2018). Common Retrieval of Aerosol Properties for Imaging Satellite Sensors. *Journal of the Meteorological Society of Japan*, *96B*, 193-209. https://doi.org/10.2151/jmsj.2018-039